Equilibrium Adsorption of Ethane, Ethylene, Isobutane, Carbon Dioxide, and Their Binary Mixtures on 13X Molecular Sieves

Sang H. Hyun and Ronald P. Danner*

Department of Chemical Engineering, The Pennsylvania State University, University Park, Pennsylvania 16802

A static, volumetric method has been used to determine the adsorption equilibria of C_2H_4, C_2H_6, i-C_4H_{10}, and CO_2 and their binary mixtures on 13X molecular sieves at various temperatures between 273 and 373 K. Pressures for the pure-component data extend up to 137.8 kPa, while all binary data were obtained at 137.8 kPa. The i-C_4H_{10}–C_2H_4 system at 298 and 323 K and the C_2H_4–CO_2 system at 298 K were found to be highly nonideal in their behavior—they exhibit adsorption azeotropes. Methods for predicting gas-mixture adsorption data from the pure-component isotherms were evaluated. Only the vacancy solution model was able to predict the azeotropic behavior even qualitatively.

Introduction

Gas adsorption on solid surfaces is an important unit operation for the separation of gases. The technology of adsorption, however, is less advanced than that of other common separation processes such as distillation, extraction, and absorption. The complexity of adsorption phenomena and the lack of accurate and complete experimental adsorption data have been major factors in inhibiting developments in adsorption technology.

Molecular sieves (zeolites) have been widely used as adsorbents because of their selectivity, adsorption capacity, and thermal and chemical stability. In practice, adsorption processing involves the treatment of multicomponent mixtures. Very few experimental data are available for adsorption systems which exhibit highly nonideal behavior. The systems reported in this paper are quite nonideal—they have adsorption azeotropes. Thus, they should be quite useful for evaluating and developing adsorption equilibrium models. Three such models are evaluated herein.

Experimental Section

Apparatus. The apparatus was of the volumetric type and used the difference technique for determining adsorbed-phase compositions. The total quantity of each gas admitted to the adsorbent and the amount of each gas remaining in the vapor phase after adsorption equilibrium had been established were determined by $P-V-T$ measurements, and an analysis of the remaining vapor phase was determined by gas chromatography. The adsorbed-phase parameters were then determined by the difference between the quantities of admitted and remaining gases. Details of the equipment and the operating procedure are described in the paper by Dorfman and Danner (*1*).

Materials. The adsorbent was molecular sieve type 13X in the form of $^1/_{16}$-in. pellets manufactured by the Linde Division of Union Carbide (Lot No. 13945390174). This sieve contained 20% by weight of an inert clay as a binding material. The unit cells of 13X molecular sieve are cubic with a large cell dimension of nearly 25 Å. The pore volume as determined by adsorption from n-pentane at 25 °C by Breck (*2*) is about 0.3 cm^3/g. The surface area determined by the BET method using nitrogen at 77 K is 525 m^2/g (*2*). For the pellets used in this study, these values had to be decreased by 20% to account for the inert binder. A differential thermal analysis of the adsorbent indicated that the water of hydration was removed at a temperature of 467 K. Thus, the solid was regenerated at a temperature above 467 K under vacuum (below 20 μmHg) for a period of at least 12 h between each run.

The C_2H_4, C_2H_6, and i-C_4H_{10} were research-grade reagents, manufactured by Phillips Petroleum Co. The purity of the C_2H_4 was 99.95 wt % with the most probable impurities being CH_4 and C_2H_6. The C_2H_6 and i-C_4H_{10} were 99.99 mol % pure. Bone-dry-grade CO_2 manufactured by Linde was used. The molecular diameters of all of the adsorbates were smaller than the window size of the molecular sieve cavities. Thus, no actual molecular sieving effect was encountered.

Pure-Gas Data

Experimental data for 12 pure-gas isotherms of C_2H_4, C_2H_6, i-C_4H_{10}, and CO_2 were collected as listed in Table I. Figure 1 shows the 323 K isotherms for these four adsorbates. No hysteresis was observed for any of these systems. The C_2H_6 and C_2H_4 isotherms are in excellent agreement with the data of Danner and Choi (*3*). Over most of the pressure range, the adsorptivity increased in the order C_2H_6, i-C_4H_{10}, C_2H_4, and CO_2.

None of these adsorbates is highly polar—only i-C_4H_{10} has any permanent dipole moment (0.1 D). However, CO_2 does have a sizable quadrupole moment which may account for its higher adsorptivity. For most of these experiments, all of the gases are above their critical temperatures except for i-C_4H_{10}, which has a critical temperature of 401.8 K. This means that the much less volatile i-C_4H_{10} is more likely to condense on the surface since it has a much larger relative saturation value (P/P°) than the other adsorbates. On the other hand, the i-C_4H_{10} has a much larger van der Waals volume (0.048 m^3/kmol) than the other gases (0.020–0.027 m^3/kmol). Thus, the i-C_4H_{10} fills the pores of the adsorbent at low pressure and then gives a horizontal isotherm. Although these observations are interesting, the state of the art in adsorption calculations is such that this type of information cannot be used directly to predict or correlate the isotherms.

Some inferences, however, can be drawn regarding the expected gas-mixture behavior based on the shapes of the pure-gas isotherms. At low pressures the i-C_4H_{10} isotherm exhibits the greatest slope and highest adsorption capacity. The CO_2 and C_2H_4 isotherms have a more gradual slope at low pressures but continue to show increases in the amount adsorbed at pressure far greater than the value at which the i-C_4H_{10} isotherm has leveled off. The C_2H_6 isotherm has an even smaller initial slope but, over the range of pressure studied, never greatly exceeds i-C_4H_{10} in terms of the amount adsorbed. Reflection on these observations suggests that at 323 K there might be an adsorption azeotrope for the i-C_4H_{10}–C_2H_4 and i-C_4H_{10}–CO_2 systems. As will be shown, this behavior was observed for the i-C_4H_{10}–C_2H_4 system. The i-C_4H_{10}–CO_2 system has not been studied.

The pure-component data were examined in terms of a number of adsorption models. The simplest model, but one which can describe type I isotherms, is that of Langmuir (*4*). This model assumes that each site on the adsorbent surface

0021-9568/82/1727-0196$01.25/0

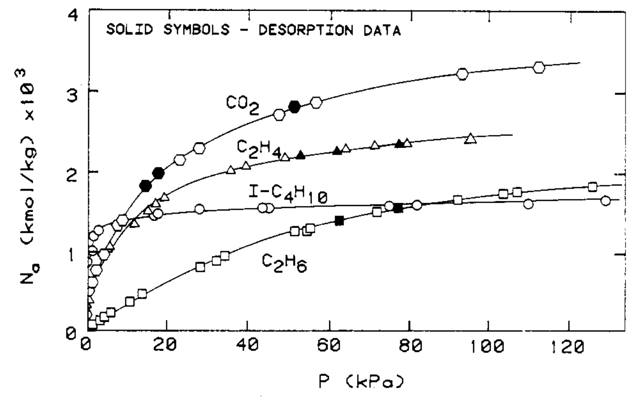

Figure 1. Pure-gas adsorption isotherms on 13X molecular sieves at 323 K.

can accommodate only one adsorbed molecule, that there are no surface heterogeneities, and that there are no interactions between adsorbed molecules. The simplified statistical thermodynamic model (SSTM) of Ruthven (*5*) and Ruthven et al. (*6*) was developed specifically for molecular sieves. It assumes that adsorbed molecules are confined within uniform cavities of the zeolite lattice but are not adsorbed at specific, localized sites; that for molecules within a particular cavity there are no attractive interactions and thus the energy of interaction is represented only by a reduction in the free volume due to the finite size of the molecules; that there are no interactions between molecules in different cavities; and that the interaction between the adsorbate molecules and solid surface is characterized by Henry's law constant. The vacancy solution model (VSM) of Suwanayuen and Danner (*7*, *8*) is based on solution thermodynamic concepts. It assumes that both the adsorbed and gas phases can be considered as solutions of adsorbates in vacancies, which are defined as the void spaces unoccupied by molecules, and that absorbate–solid and adsorbate–adsorbate interactions can be accounted for by activity coefficients. The ideal adsorbed solution model (IASM) of Myers and Prausnitz (*9*) is also based on solution thermodynamic concepts, but it assumes that the adsorbed solutions are ideal and sets all activity coefficients to unity. While the VSM can correlate pure-gas data and predict gas-mixture data, the IASM does not provide a means of correlating pure-gas behavior.

The Langmuir model, the SSTM, and the VSM did reasonably well in correlating the isotherms. The VSM, however, gave the least average deviation. For each of the models, one can calculate the isosteric heat of adsorption if data for a number of different temperatures are available. The results of this exercise are given in Table II. The reference values of the heats of adsorption were determined for C_2H_4 and C_2H_6 by Kiselev and Yashin (*10*) using a chromatographic technique, and that for CO_2 was obtained by Huang and Zwiebel (*11*) using a calorimetric unit. The VSM values are in closer agreement with the reference values than either of the other two methods.

Gas-Mixture Adsorption Data

Binary gas-mixture adsorption data were obtained on 13X molecular sieves at a constant total pressure of 137.8 kPa and temperatures of 298, 323, and 373 K for the i-C_4H_{10}–C_2H_4 system, and temperatures of 298 and 323 K for the i-C_4H_{10}–C_2H_6 and C_2H_4–CO_2 systems. The experimental data for the equilibrium vapor- and adsorbed-phase compositions and the total amounts adsorbed are presented in Table III. The adsorption phase diagrams for the i-C_4H_{10}–C_2H_4 systems at 298 and 373 K and the i-C_4H_{10}–C_2H_6 and C_2H_4–CO_2 systems at 298 K are shown in Figure 2.

As expected the i-C_4H_{10}–C_2H_4 systems at 298 and 323 K (data at 323 K are given in Figure 3) have adsorption azeotropes. No azeotrope is apparent at 373 K. Similarly the C_2H_4–CO_2 system at 298 K exhibited an azeotrope at 0.09 mole fraction C_2H_4, but at 323 K no azeotrope was observed.

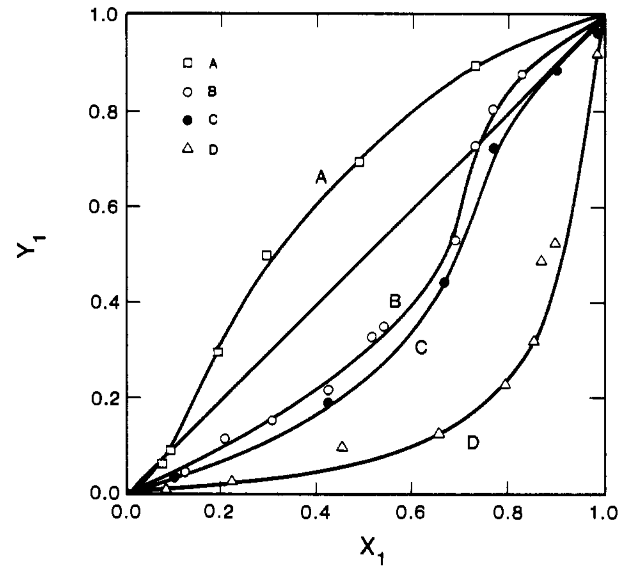

Figure 2. Adsorption phase diagrams for binary mixtures on 13X molecular sieves at 137.8 kPa: (A) C_2H_4 (1)–CO_2 (2) at 298 K; (B) i-C_4H_{10} (1)–C_2H_4 (2) at 298 K; (C) i-C_4H_{10} (1)–C_2H_4 (2) at 373 K; (D) i-C_4H_{10} (1)–C_2H_6 (2) at 298 K.

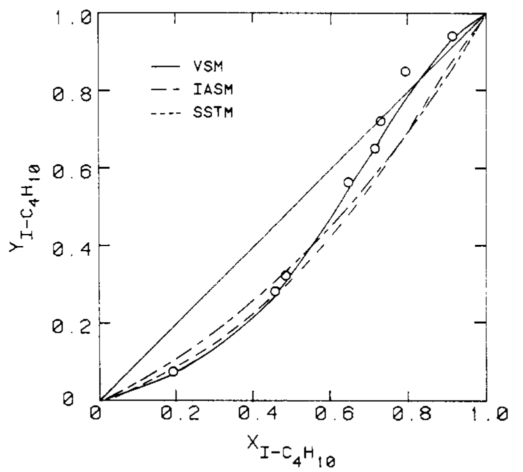

Figure 3. Predictions of the adsorption equilibrium phase diagram for i-C_4H_{10}–C_2H_4 mixtures on 13X molecular sieve at 323 K and 137.8 kPa.

Figure 2 also graphically depicts the marked difference between i-C_4H_{10}–C_2H_4 and i-C_4H_{10}–C_2H_6 systems at the same temperature and total pressure. In mixtures with C_2H_6, i-C_4H_{10} has a strong preference for the adsorbed phase throughout the entire composition range, while the preferentially adsorbed component shifts at the azeotropic point in the case of the i-C_4H_{10}–C_2H_4 system. Although not shown in Figure 2, the 323 K phase diagram for the i-C_4H_{10}–C_2H_6 system was almost identical with the 298 K diagram.

The behavior of the total amounts adsorbed is shown in Figure 4 for the i-C_4H_{10}–C_2H_4 systems at the three temperatures. As the temperature increases, the total amount adsorbed decreases as expected. At the lower temperatures the total amount adsorbed is more sensitive to the equilibrium composition than at the higher temperature. This behavior is also true for the i-C_4H_{10}–C_2H_6 system but was not apparent for the C_2H_4–CO_2 system.

The adsorption models used to fit the pure-component data were evaluated for their ability to predict the binary-adsorption behavior using the pure-component information. The spreading pressures needed for the IASM (*9*) were obtained by integrating

Table I. Pure-Gas Adsorption Data

ethylene		ethane		isobutane		carbon dioxide	
p^b	$10^3N_a{}^c$	p^b	$10^3N_a{}^c$	p^b	$10^3N_a{}^c$	p^b	$10^3N_a{}^c$
T = 298.15 K							
0.24	0.41	0.54	0.04	0.20	0.75	0.24	0.44
0.27	0.41	1.05	0.09	0.24	0.99	0.37	0.61
0.34	0.41	1.21	0.11	0.47	1.04	0.78	0.74
0.57	0.58	3.54	0.27	1.52	1.36	0.88	0.93
0.61	0.41	7.54	0.51	5.23	1.48	2.16	1.19
0.81	0.69	9.71	0.66	7.38	1.49	2.39	1.28
1.15	0.83	10.05	0.69	12.37	1.62	2.80	1.40
1.31	0.89	10.40	0.70	13.12	1.63	3.78	1.57
1.55	0.87	13.55[a]	0.91	23.00	1.63	7.25	2.02
1.59	0.94	14.00	0.99	23.97[a]	1.71	8.26	2.16
1.62	0.97	16.72[a]	1.04	26.37	1.71	15.91	2.68
1.85	1.01	20.00[a]	1.20	40.90	1.79	22.19[a]	2.99
3.07	1.29	20.94	1.24	57.46	1.84	23.16	3.02
3.20	1.31	23.64	1.34	76.64	1.82	29.74[a]	3.19
3.91	1.36	24.82[a]	1.39	90.50	1.81	45.79	3.44
3.98	1.43	33.09[a]	1.62	137.84	1.88	54.86	3.60
4.65	1.54	40.94[a]	1.74			72.76	3.71
5.60	1.64	43.05	1.79			87.25	3.84
5.70	1.63	46.53	1.85			102.32	3.92
7.99	1.80	50.14	1.90			137.84	4.02
10.86	1.95	50.75[a]	1.90				
23.40	2.31	54.46	1.97				
29.98	2.41	63.69[a]	2.02				
40.80	2.52	68.38	2.07				
56.65[a]	2.65	71.18[a]	2.06				
70.17[a]	2.70	80.05	2.10				
88.98	2.76	84.26[a]	2.15				
94.41	2.76	94.21	2.20				
116.19	2.81	110.83	2.25				
137.84	2.81	124.66	2.28				
		137.84	2.29				
T = 323.15 K							
0.67	0.25	2.12	0.08	0.40	0.70	0.44	0.21
0.74	0.28	4.25	0.15	0.78	0.86	1.11	0.49
0.94	0.38	5.26	0.16	1.48	1.00	1.59	0.60
1.79	0.56	6.24	0.19	2.43	1.19	2.50	0.76
1.85	0.57	14.23	0.44	2.66	1.25	4.68	0.97
3.00	0.70	28.29	0.79	8.13	1.37	7.76	1.34
4.32	0.90	32.51	0.87	17.20	1.43	8.63	1.41
5.60	0.97	34.06	0.92	17.43	1.46	15.11[a]	1.84
5.66	1.01	52.16	1.26	29.13	1.52	17.97[a]	1.97
6.71	1.03	55.00	1.28	43.97	1.55	23.37	2.14
12.04	1.35	55.23	1.28	45.45	1.55	28.36	2.29
15.58	1.49	63.22[a]	1.39	75.02	1.59	47.61	2.71
17.10	1.58	72.76	1.49	81.80	1.59	51.93[a]	2.80
19.56	1.67	78.43[a]	1.55	110.60	1.60	57.22	2.87
36.21	2.02	92.49	1.66	130.22	1.64	94.06	3.22
39.65	2.07	104.29	1.73	137.84	1.65	113.09	3.30
49.77	2.18	107.53	1.76			137.84	3.44
53.38[a]	2.22	126.82	1.86				
62.88[a]	2.28	134.90	1.88				
65.04	2.29	137.84	1.89				
72.23	2.33						
78.53[a]	2.37						
79.61	2.37						
95.93	2.43						
137.84	2.50						
T = 373.15 K							
1.05	0.07	3.30	0.03	0.64	0.17		
1.31	0.12	9.88	0.08	1.01	0.23		
1.85	0.13	11.70[a]	0.11	1.69	0.46		
2.70	0.18	16.32	0.15	1.72	0.47		
3.78	0.24	17.84[a]	0.16	3.24	0.69		
5.77	0.32	18.24	0.16	4.52	0.82		
6.95	0.38	25.59	0.22	10.42	1.03		
12.71	0.55	32.77[a]	0.28	14.33	1.08		
18.28	0.69	37.06	0.32	14.80	1.10		
19.12	0.74	37.19	0.32	16.08[a]	1.08		
25.15	0.87	39.35[a]	0.34	27.65	1.21		
32.40	0.97	46.87[a]	0.39	32.66	1.23		
42.08	1.10	51.18	0.42	40.66	1.26		
43.23	1.10	55.57[a]	0.45	64.57	1.33		
45.05	1.13	56.24	0.46	80.57	1.33		
46.53	1.14	56.98	0.47	107.16	1.33		

Table I (*Continued*)

ethylene		ethane		isobutane		carbon dioxide	
p[b]	10^3N_a[c]	p[b]	10^3N_a[c]	p[b]	10^3N_a[c]	p[b]	10^3N_a[c]
51.12	1.20	61.00[a]	0.50	137.84	1.34		
56.12	1.26	66.16[a]	0.52				
61.37[a]	1.32	74.58[a]	0.59				
61.77	1.33	80.52	0.61				
63.29	1.35	85.24	0.66				
69.93	1.39	87.40[a]	0.67				
70.88[a]	1.40	88.65	0.67				
81.19	1.47	100.38[a]	0.74				
87.53	1.53	121.35	0.86				
93.57	1.55						
96.07[a]	1.55						
126.11	1.72						
137.84	1.74						

Ethane, $T = 273.15$ K

P	10^3N_a	P	10^3N_a	P	10^3N_a	P	10^3N_a
			$T = 273.15$ K				
0.40	0.12	12.11[a]	1.70	20.64	2.05	61.81[a]	2.47
0.84	0.19	13.52	1.77	29.61	2.24	65.25	2.50
1.15	0.23	14.23[a]	1.81	34.53[a]	2.29	73.14	2.53
2.46	0.42	16.22	1.90	47.54	2.41	75.90	2.52
3.20	0.64	16.89	1.93	48.93	2.41	87.77	2.58
4.52	0.86	17.03[a]	1.94	56.63	2.46	97.04	2.61
8.30	1.35	19.15	2.02	59.28	2.49		

[a] Desorption points. [b] In kPa. [c] In kmol/kg.

Table II. Isosteric Heats of Adsorption for the Pure Gases on Molecular Sieve Type 13X

	10^6(isosteric heat of adsorption), J/kmol			
adsorbate gas	Langmuir model	SSTM[a]	VSM[b]	ref value
C_2H_4	27.91	35.75	40.12	38.10
C_2H_6	29.22	32.22	26.71	25.12
$i\text{-}C_4H_{10}$	39.31	43.13	58.93	
CO_2	34.44	33.57	70.67	76.62

[a] Simplified statistical thermodynamic model (5). [b] Vacancy solution model (6).

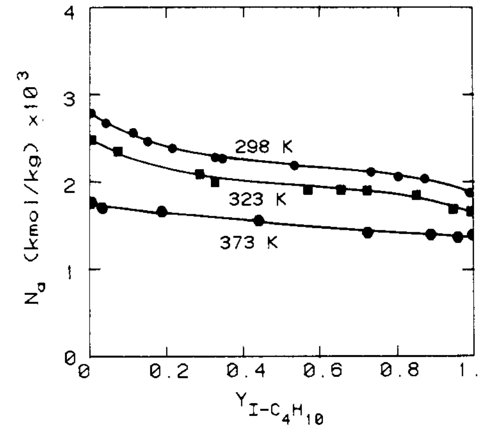

Figure 4. Total amount adsorbed from binary mixtures of $i\text{-}C_4H_{10}$–C_2H_4 on 13X molecular sieves at 137.8 kPa.

Table III. Gas-Mixture Adsorption Data[a]

Y_1	X_1	10^3N_a	Y_1	X_1	10^3N_a
		Isobutane (1)–Ethylene (2) at 298.15 K			
4.50	12.23	2.68	34.85	53.78	2.27
11.68	20.85	2.63	53.10	68.97	2.19
15.15	30.86	2.46	73.02	72.74	2.14
21.63	42.37	2.39	80.47	76.60	2.07
32.49	51.61	2.30	87.45	82.18	2.05
		Isobutane (1)–Ethylene (2) at 323.15 K			
7.76	18.63	2.37	65.33	71.16	1.92
28.43	45.75	2.13	72.23	73.16	1.93
32.37	48.55	2.00	85.66	79.59	1.87
56.75	64.06	1.90	94.93	91.78	1.67
		Isobutane (1)–Ethylene (2) at 373.15 K			
3.39	10.21	1.74	72.79	76.44	1.47
18.76	42.27	1.68	88.39	89.62	1.40
44.25	66.16	1.57	96.17	98.32	1.38
		Isobutane (1)–Ethane (2) at 298.15 K			
0.30	8.29	2.26	31.84	84.87	1.96
2.69	21.94	2.18	48.68	86.54	1.93
9.96	45.14	2.05	52.23	89.47	1.93
12.70	65.40	1.96	92.00	97.90	1.91
22.98	79.03	1.95	96.32	99.76	1.91
		Isobutane (1)–Ethane (2) at 323.15 K			
3.47	36.25	1.84	65.29	92.18	1.67
3.69	27.71	1.83	81.90	97.42	1.68
12.23	63.53	1.75	89.05	99.46	1.67
21.14	80.17	1.68			
		Ethylene (1)–Carbon Dioxide (2) at 298.15 K			
6.56	7.52	3.98	49.30	29.63	3.65
9.01	9.01	3.93	69.68	48.19	3.35
29.32	18.97	3.78	88.94	72.77	3.07
		Ethylene (1)–Carbon Dioxide (2) at 323.15 K			
9.43	8.66	3.41	68.23	58.00	2.88
30.43	26.61	3.29	90.04	83.41	2.66
60.19	47.35	3.00			

[a] Y = vapor-phase mole percent; X = adsorbed-phase mole percent; N_a = total kilomoles adsorbed per kilogram of 13X molecular sieves; P = 137.8 kPa.

the VSM (*7*, *8*) isotherm equation. Of particular interest was the ability of these models to predict the nonideal, azeotropic behavior observed. Figure 3 shows the predictions for the $i\text{-}C_4H_{10}$–C_2H_4 system on molecular sieve 13X at 323 K. The IASM and the SSTM do not predict an azeotrope, while the VSM does although not with high accuracy. None of the models predict the slight azeotropic behavior found experimentally in the C_2H_4–CO_2 system at 298 K. Suwanayuen and Danner (*8*) described a semiempirical means of using the isosteric heats of adsorption to account for adsorbate–adsorbate interactions. Use of the method for the $i\text{-}C_4H_{10}$–C_2H_4 system caused the VSM to predict more pronounced azeotropic behavior, but the quantitative agreement with the data was poorer. This suggests, however, that further developments in calculating the activity coefficients in the VSM could lead to improved quantitative results. The SSTM assumes that the only interactions between adsorbed molecules are those due to molecular size difference. Since this difference is not dependent on composition, one would not expect that the SSTM could predict azeotropic behavior. The ideality assumptions inherent in the IASM also preclude it from predicting azeotropes.

Glossary

N_a	amount adsorbed (kmol/kg)
P	adsorption equilibrium pressure (kPa)
P°	vapor pressure at the adsorption temperature (kPa)
X_i	mole fraction of component *i* in the adsorbed phase
Y_i	mole fraction of component *i* in the bulk gas phase

Literature Cited

(1) Dorfman, L. R.; Danner, R. P. *AIChE Symp. Ser. No. 152* **1975**, *71*, 30.
(2) Breck, D. "Zeolite Molecular Sieves"; Wiley: New York, 1974.
(3) Danner, R. P.; Choi, E. C. F. *Ind. Eng. Chem. Fundam.* **1978**, *17*, 248.
(4) Langmuir, I. *J. Am. Chem. Soc.* **1918**, *40*, 1361.
(5) Ruthven, D. M. *Nature (London), Phys. Sci.* **1971**, *232*, 70.
(6) Ruthven, D. M.; Loughlin, K. F.; Holborow, K. A. *Chem. Eng. Sci.* **1973**, *28*, 701.
(7) Suwanayuen, S.; Danner, R. P. *AIChE J.* **1980**, *26*, 68.
(8) Suwanayuen, S.; Danner, R. P. *AIChE J.* **1980**, *26*, 76.
(9) Myers, A. L.; Prausnitz, J. M. *AIChE J.* **1965**, *11*, 121.
(10) Kiselev, A. V.; Yashin, Y. I. "Gas Adsorption Chromatography"; Plenum Press: New York, 1969.
(11) Huang, A. A.; Zweibel, I. "Heats of Adsorption of CO_2 and SO_2 on Molecular Sieves", paper presented at 3rd International Conference on Molecular Sieves, Zurich, Switzerland, Sept 1973.

Received for review April 24, 1981. Accepted January 15, 1982. Financial support from Air Products and Chemicals, Inc., is gratefully acknowledged.

Densities and Viscosities of Solutions of $Cd(NO_3)_2$ in a Solvent $(Ag,Tl)NO_3$

Marie-Christine Abraham and Maurice Abraham*

Département de Chimie, Université de Montréal, C.P. 6210, Succursale A, Montréal, Québec, Canada H3C 3V1

James Sangster

Département de Génie Métallurgique, Ecole Polytechnique, Campus de l'Université de Montréal, C.P. 6079, Succursale A, Montréal, Québec, Canada H3C 3A7

Densities and viscosities of the mixed liquid melt $AgNO_3$ + $TlNO_3$ + $Cd(NO_3)_2$ have been measured in the temperature range 353–393 K. The Ag/Tl mole ratio was fixed at 1.06, and the mole fraction X_{Cd} of $Cd(NO_3)_2$ in the solution was varied between 0 and 0.1. The molar volume of the solution is a linear function of both the temperature and X_{Cd}. The viscosity of the solution follows an Arrhenius relation $\eta = A\exp(E/RT)$ in which both ln *A* and *E* were found to be linear functions of X_{Cd}: $\ln A(\mathrm{cP}) = -13.30X_{Cd} - 5.67$; $E = 59.680X_{Cd} + 27.142$ kJ mol^{-1}.

Introduction

The viscosity of fused salts is not usually, if ever, measured with great precision, simply because of the experimental difficulties associated with high temperatures. When practical application requires the use of certain salts rather than others, the operating temperature cannot be chosen arbitrarily. This is not the case, however, when one wishes to test physicochemical models or theories (*1*, *2*); one can then choose systems allowing lower operating temperatures, with consequently greater precision. With this in mind, certain low-melting nitrate mixtures lend themselves to systematic investigation by experimental methods most often used at ordinary temperatures. An example is the mixed melt $AgNO_3$ + $TlNO_3$ + $Cd(NO_3)_2$ in certain concentration ranges (*3*), and in this article we present the results of measurements of the viscosity and the density of this system under the following conditions:

$$X_{Cd(NO_3)_2} \le 0.1$$

$$X_{AgNO_3}/X_{TlNO_3} = 1.06$$

in the temperature range 95–130 °C.

Experimental Section

$AgNO_3$ (A.C.S., Johnson Mathey) was used as received. $TlNO_3$ (Alfa) was recrystallized 3 times in water, filtered, and dried at 120 °C in vacuo. $Cd(NO_3)_2$ was introduced into the mixture as $Cd(NO_3)_2\cdot 4H_2O$ (Fisher Certified). The fused nitrates were heated in vacuo to 200 °C, to drive off water without decomposition, and then filtered through sintered glass. The mixtures were kept, for periods never exceeding 2 weeks, in a hot air oven at 150 ° in the absence of light.

The densities were measured with a 25-cm^3 Pyrex volumetric flask, calibrated twice with bromobenzene (Fisher Scientific Co., Certified) (*4*) at each experimental temperature. The uncertainty of this calibration was ±0.005 cm^3. The flask was placed in a thermostated oil bath regulated to ±0.05 °C. The level of liquid in the flask was observed horizontally with a magnifying glass through the glass wall of the bath and adjusted at each experimental temperature by means of liquid from a preheated pipet. Temperature was measured with ERTCO certified thermometers (Ever Ready Thermometer Co.). To check this pycnometric method, measurements were made on water between 80 and 100 °C, the density being known with particular precision (*5*). The results were within 0.03% of the published values, which indicates that the method is entirely satisfactory for the fused salt systems of the present work.

Viscosities were measured with an Ostwald-Ubbelhode viscometer (Cannon Instrument Co.). Its constant, *C*, was approximately 0.01 cSt s^{-1}. The flow times, *t*, lay in the range 300–1000 s, and the measured viscosities in the range 10–40 cP. The kinetic energy correction thus was negligible, and the kinematic viscosity ν was given by

$$\nu = Ct \qquad (1)$$

The absolute viscosity is given by

$$\eta = \nu\rho \qquad (2)$$

0021-9568/82/1727-0200$01.25/0